

SCHOTTKY BARRIER JUNCTIONS OF HYDROGENATED AMORPHOUS SILICON-GERMANIUM ALLOYS

Hideharu MATSUURA, Hideyo OKUSHI and Kazunobu TANAKA

Electrotechnical Laboratory, 1-1-4 Umezono, Sakura-mura, Niihari-gun,
Ibaraki 305, Japan

The current-transport mechanisms of Au/a-SiGe:H junctions have been investigated. It has been found that electrons are transported by multi-step tunneling through a part of the Schottky barrier, which can be explained by the "diffusion-field-emission" model. The existence of tunneling process has also been confirmed by the temperature dependence of isothermal-capacitance-transient-spectroscopy (ICTS) signals. The bump of DOS in a-SiGe:H has been found to be located at about 0.4 eV below the conduction band edge.

1. INTRODUCTION

Hydrogenated amorphous silicon-germanium alloys (a-Si_{1-x}Ge_x:H) have recently been applied to enhance the conversion efficiency of amorphous solar cells. However, there have been few reports on the junction transports of a-Si_{1-x}Ge_x:H. In this work, we propose a new model for the carrier transport in amorphous Schottky barrier junctions. We prepared Au/a-Si_{1-x}Ge_x:H Schottky barrier junctions under various deposition conditions¹ and discuss their current density vs. voltage (J-V) characteristics as well as the transient capacitance using our new model. The density of states (DOS) has also been determined by isothermal capacitance transient spectroscopy (ICTS)².

2. THEORY

Since, in crystalline semiconductors, electron collisions in the depletion region can be neglected, the thermionic-emission theory can be applied to their Schottky barrier junctions. Figure 1(a) shows schematically the possible transport channels for electrons across the Schottky barrier of an n-type crystalline

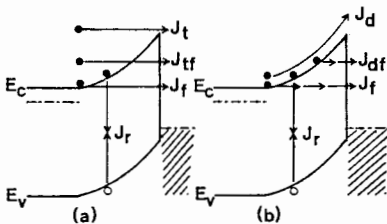


FIGURE 1

Band diagrams for Schottky barrier junctions. (a) metal/n-type crystalline and (b) metal/n-type amorphous.

semiconductor under the forward bias; the thermionic-emission current J_t , the thermionic-field-emission current J_{df} , the field-emission current J_f , and the recombination current J_r .

In amorphous semiconductors, on the other hand, electron collisions in the depletion region should be taken into account when the transport is discussed, because a higher density of defect states

lies in the gap over a wider energy range. This means that the diffusion current J_d is more important in amorphous Schottky barrier junctions, which was experimentally demonstrated in our earlier work³. In actual amorphous Schottky barrier junctions, besides J_d , J_r and the tunneling currents of J_{df} and J_f via localized states in the depletion region also flow across the Schottky barrier, as is shown in Fig. 1(b). The diffusion-field-emission current J_{df} can be described by⁴

$$J_{df} \propto \exp(V/E_0), \quad (1)$$

with

$$E_0 = E_{00} \coth(qE_{00}/kT) \quad (2)$$

and

$$E_{00} = (1+\gamma)(h/4\pi)(N_1/m^* \epsilon)^{1/2}, \quad (3)$$

where V is the forward-biased voltage, N_1 the effective density of the gap states which can be graphically obtained from the slope of $1/C^2$ - V characteristics, and γ the multi-step tunneling factor. In case the density of localized states is considerably high, the field-emission current J_f becomes dominant, which is given by⁴

$$J_f \propto \exp(V/E_{00}). \quad (4)$$

3. RESULTS AND DISCUSSION

3.1. J-V Characteristics

Undoped and phosphorus-doped a-Si_{1-x}Ge_x:H films were deposited by the glow-discharge decomposition of GeH₄/SiH₄ and GeH₄/SiH₄/PH₃ gas mixtures, respectively, under three different conditions ("Diode" films: using a conventional diode-type reactor, "Triode" films: using a triode-type reactor with a mesh electrode between the anode and the cathode, and "H₂-dilution" films: using the triode-type reactor and H₂-diluted starting gas materials). All of these films have the optical gap of about 1.5 eV and the atomic ratio of Ge/(Si+Ge) in those films is about 55%. J-V characteristics of Au/a-Si_{1-x}Ge_x:H junctions were measured as a function of temperature over the range between 151 and 295 K.

Poor rectifying properties were observed for "Diode" films probably due to the high density of localized states, while the Schottky barrier junctions of "Triode" and "H₂-dilution" films exhibited good rectifying properties. It was found that the forward current of Y4 (905-ppm PH₃) of "Triode" films obeyed Eq. (4), i.e., J_f , while those of Z2 (7.8-ppm PH₃) and Z4 (1080-ppm PH₃) of "H₂-dilution" films were expressed by Eq. (1) of J_{df} .

The values of E_{00} obtained from their J-V characteristics were 3.1×10^{-2} , 1.7×10^{-2} and 2.3×10^{-2} eV for Y4, Z2 and Z4, respectively. However, E_{00} can independently be estimated by Eq. (3) using the experimental values of N_1 . Since N_1 of the samples of Y4, Z2 and Z4 was obtained from their $1/C^2$ - V

relationships as 1.4×10^{17} , 2.4×10^{16} and $1.5 \times 10^{17} \text{ cm}^{-3}$, E_{00} was then estimated to be 1.8×10^{-3} , 7.2×10^{-4} and $1.8 \times 10^{-3} \text{ eV}$, respectively, if one-step tunneling ($\gamma=0$) is assumed. In this estimation, $\epsilon=16\epsilon_0$ and $m^*=m_0$ were used, where ϵ_0 is the free-space permittivity and m_0 the free electron mass. The above values are much smaller than those obtained from the J-V characteristics. This estimation gap does essentially exist even when $m^*=0.1m_0$ is used, suggesting that the assumption of one-step tunneling in Eq. (3) is wrong. Consequently, it is reasonable to consider that the multi-step tunneling is dominant in those amorphous Schottky barrier junctions.

Next, we discuss the difference in observed electron transport between Y4 dominated by J_f and Z4 dominated by J_{df} . The value of E_{00} of Y4 obtained from the J-V characteristics was larger than that of Z4. The dark conductivities of the films of Y4 and Z4 were 1.5×10^{-5} and $1.9 \times 10^{-4} \text{ S/cm}$, the photoconductivities were 5.3×10^{-5} and $5.3 \times 10^{-4} \text{ S/cm}$, and B-values obtained from T_{auc} plots were 670 and 830 $\text{eV}^{-1/2} \text{ cm}^{-1/2}$, respectively. However, the width of the depletion region may be nearly the same in both, since the values of N_t of the samples are nearly equal. The tail states above the valence band edge (E_v) determined by the photoacoustic spectroscopy were also similar to each other. The difference in junction properties between those samples characterized by J_f and J_{df} seems to come from the tail-state distribution below the conduction band edge (E_c), which determines a characteristic energy at which tunneling of electrons start, namely, J_f or J_{df} dominates.

3.2. Transient Capacitance

In order to get more detailed information on the transport for electrons as well as the DOS distribution of each material, we made ICTS measurements on P-doped $a\text{-Si}_{1-x}\text{Ge}_x\text{:H}$. Figure 2 shows the DOS distributions of Y4, Z3 (77-ppm PH_3) and Z4 deduced from the ICTS spectra ($S(t)$) using the following equations²:

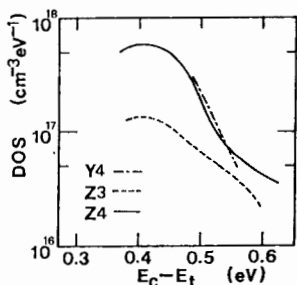


FIGURE 2
DOS distributions of P-doped
 $a\text{-SiGe:H}$.

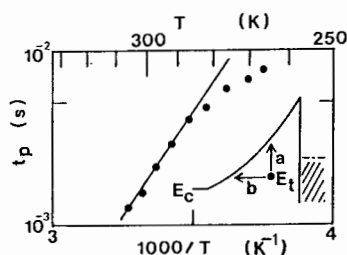


FIGURE 3
Temperature dependence of t_p
for the specimen Z4.

$$S(t) = d(\ln(C(t)^2))/d(\ln(t)), \quad (5)$$

$$E_c - E_t = kT \ln(\sigma_n v_{th} N_C t), \quad (6)$$

where $C(t)$ is the transient capacitance at time (t), σ_n the electron-capture cross section at E_t and v_{th} the thermal velocity. The voltage-pulse-width dependence² of $S(t)$ gives σ_n at each E_t . As shown in the figure, the energy location of the maximum of the DOS distribution is located at 0.41 eV below E_c independent of the doping level.

We have determined the energy location of the maximum of the DOS distribution using a different method. The temperature dependence of the time (t_p) given the maximum of $S(t)$ was measured. The result is shown in Fig. 3, and 0.45 eV was obtained as the activation energy of t_p in the temperature range between 287 and 306 K, being nearly equal to the maximum position ($E_c - E_t$) of the DOS distribution determined by the voltage-pulse-width dependence. This indicates that σ_n is nearly constant in this higher temperature region.

In the lower temperature region ($T < 287$ K), however, t_p seems to be saturated as T decreases. To explain this effect, σ_n in Eq.(6) should increase as T decreases. In the present stage, however, no model can uniquely explain the temperature dependence of the capture cross section, where it increases as T decreases below 287 K but stays constant above 287 K. Our diffusion-field-emission model suggests that, besides the ordinary thermal emission process indicated by (a) in the figure, the tunneling process by field emission indicated by (b) affects t_p . Since the tunneling process is independent of temperature, it is dominant compared with the thermal emission process at low temperatures.

4. CONCLUSIONS

The multi-step tunneling is considered to be a dominant mechanism in the electron transport of Au/a-Si_{1-x}Ge_x:H junctions. It is suggested that this process affects ICTS signals at lower temperatures. The DOS distributions for P-doped a-Si_{1-x}Ge_x:H obtained by ICTS at room temperature have a maximum at around 0.4 eV below E_c .

REFERENCES

- 1) A. Matsuda, M. Koyama, N. Ikuchi, Y. Imanishi, and K. Tanaka, Jpn. J. Appl. Phys. 25 (1986) L53.
- 2) H. Okushi, Phil. Mag. B52 (1985) 33.
- 3) H. Matsuura, A Matsuda, H. Okushi, and K. Tanaka, J. Appl. Phys. 58 (1985) 1578.
- 4) H. Matsuura and H. Okushi, J. Appl. Phys. 62 (1987) 2871.